

Supersonic Combustion using Multiple Stinger-shaped Injectors*

Toshinori KOUCHI,^{1)†} Sadatake TOMIOKA,²⁾ Kohshi HIRANO,^{3)‡} Akiko MATSUO,³⁾ and Goro MASUYA⁴⁾

¹⁾Department of Mechanical and System Engineering, Okayama University, Okayama 700–8530, Japan

²⁾Research and Development Directorate, Japan Aerospace Exploration Agency, Kakuda, Miyagi 981–1525, Japan

³⁾Department of Mechanical Engineering, Keio University, Yokohama, Kanagawa 223–8522, Japan

⁴⁾Center for Education and Research on Science for Global Safety, Tohoku University, Sendai, Miyagi 980–8579, Japan

Key Words: Fuel Mixing, Combustor Performance, Supersonic Mixing and Combustion, Scramjet Engine

Nomenclature

D : (equivalent) injector diameter

J : jet-to-crossflow momentum-flux ratio

s : interval between injectors

P : pressure

x, y, z : stream-, span-, height-wise directions

ϕ : local fuel equivalence ratio

Φ : bulk fuel equivalence ratio

η_c : local combustion efficiency

Subscripts

0: stagnation condition

CR: circular case

ST: stinger case

W: values on wall

1. Introduction

The scramjet engine is a promising candidate for propulsion systems applied for future aerospace transportation. The fuel injection system is a key technology for realizing scramjets. One of the major concerns about the injection systems is how to make fuel penetrate the entire combustor cross-section.

The port geometry of the injector^{1–7)} is one of the important factors for fuel penetration. Some injector shapes improve the fuel penetration by reducing the effective back pressure around the injectors.^{2,3,8)} Recently, we developed a stinger-shaped injector (stinger injector). The injector has a very high length-to-width ratio slit with a sharp leading-edge⁸⁾ and achieves a higher fuel penetration ratio. We experimentally confirmed that the performance of a combustor with a stinger injector installed is much higher than that with a conventional circular injector.^{9,10)} In the series of experiments, we only considered single-injector configurations.

A realistic scramjet combustor would require multiple injectors oriented normal to a supersonic stream to spread the

fuel evenly along the lateral plane. Additional fuel injection to either side of the single injector changes the downstream mixing^{11–14)} because the fuel jets from adjacent injectors interact with each other.

For a non-reactive case, Rogers¹³⁾ investigated hydrogen fuel concentrations of multiple circular injections for two injector spacings of 6.25 and 12.5 injector diameters. He concluded that the injector spacing affects the fuel penetration less, but it greatly affects the uniformity of the fuel distributions and the mixing efficiency. Sun et al.¹⁴⁾ obtained similar results using a laser visualization technique and CFD. For multiple injections at a spacing of 10 injector diameters, each jet separately developed downstream. On the other hand, the bow shock waves upstream of the injectors connected to each other and the air entering between the adjacent injectors was not enough to achieve a higher mixing efficiency for a smaller injector spacing of 5 injector diameters.

Although there are some studies focusing on the effects of multiple injections for fuel mixing in non-reactive cases, there is no research focused on the effects to supersonic combustion even for circular injector shapes. Therefore, we conducted experiments using a supersonic combustor with multiple stinger injectors, and measured the local equivalence ratio and combustion efficiency at the exit of the combustor. The results were compared with those from experiments using multiple circular injectors. We also discuss the difference between combustor performance using multiple injectors and that using a single injector.

2. Experimental Apparatus and Data Reduction

2.1. Wind tunnel facility

Figure 1 illustrates the blow-down, direct-connect combustor test facility used for this study. The facility provided a Mach 2.44 supersonic vitiated airflow from the facility nozzle. Stagnation pressure (P_0) and temperature of the flow were 1.05 ± 0.02 MPa and 2060 ± 60 K, respectively. The oxygen mole fraction of the flow was 21.0 ± 1.0 vol.%. The combustor was equipped with an injector block assembly on the bottom wall in the constant-area section. We used a Cartesian coordinate system, with the origin at the center of the injector block, the stream-wise direction on the x -axis, the span-wise direction from the centerline of the combustor on

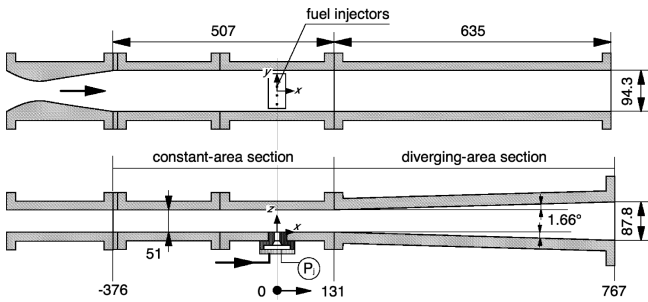


Fig. 1. Schematic diagram of supersonic combustor.

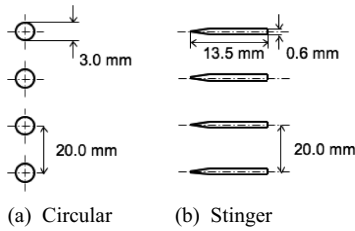


Fig. 2. Schematic diagram of multi-injection orifices: (a) circular and (b) stinger shape. Fuel is injected in the direction perpendicular to the paper, while crossflow air travels left to right.

the y -axis and the height direction from the injector wall on the z -axis. Injection pressure and fuel mass flow rate were monitored for evaluating jet-to-freestream momentum flux ratio (J) and bulk fuel equivalence ratio (Φ). Hydrogen fuel at room temperature was injected perpendicularly through four sonic orifices to the crossflow.

Figure 2 depicts the two different multiple injectors: (a) conventional circular port with diameter (D) of 3 mm and (b) stinger port with equivalent diameter (also D) of 3 mm. The geometrical shape of each stinger port is the same as the previous one.⁸⁻¹⁰ The center-to-center spacing of the injectors (s) was set to be 20 mm with the four injectors oriented to have equal spacing for the combustor width (94.3-mm-width/5 intervals for 4 injectors). This corresponded to $s/D \sim 6.7$. For this interval regime, the multiple jets from the adjacent injectors are expected to interact with each other,^{13,14} so multiple injections would alter the downstream mixing and combustion. The overall discharge coefficient of the circular injector was 0.82 and that of the stinger injector was 0.69. Note that $\Phi \sim 0.15$ corresponds to J of unity for the stinger injector array.

2.2. Measurements

We measured wall pressure (P_W) distributions on the injector-side and opposite-side walls using mechanical scanning pressure sensors. To determine the benefit of the stinger injector, the pressure distribution in the stinger case was divided by that in the circular case. We refer to this pressure ratio ($P_{W,ST}/P_{W,CR}$) as the pressure gain of the stinger injector. The pressure gains were measured with an overall uncertainty of $\pm 4\%$. In addition to pressure, we sampled exhaust gas at the exit of the combustor using a water-cooled, reaction-quenching sampling probe¹⁵ to evaluate the local equivalence ratio (ϕ) and combustion efficiency (η_c). There were

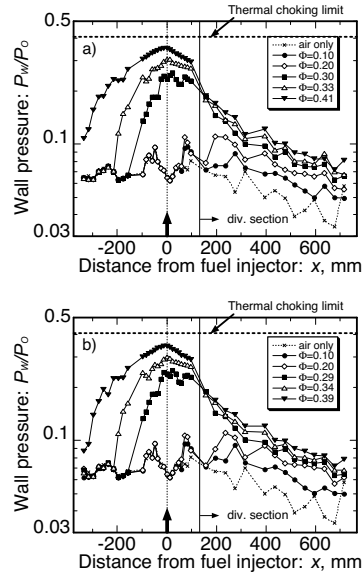


Fig. 3. Wall pressure distributions using (a) multiple circular injectors and (b) multiple stinger injectors at various Φ .

63 sampling points with an interval of 10 mm (9 points in the height direction, 7 in the width direction). The data at the same $|y|$ positions were averaged assuming symmetry with the $y = 0$ mm plane and displayed as a contour map in the half yz -plane. The discrepancy in the data at the same $|y|$ positions was about 15% in each local value. The local ϕ included fuel consumed by combustion. The local η_c is the ratio of the amount of fuel actually burned to the amount available for reaction. The typical uncertainty in ϕ is 2% and that in η_c is 3% around ϕ of unity. See Kouchi et al.⁹ for details on the measurements and their uncertainties.

3. Results and Discussions

3.1. Wall pressure distributions and pressure gain

Figures 3(a) and (b) plot the P_W distributions using the multiple circular and stinger injectors for various Φ . For the circular case, the combustion region was limited in the diverging section for $\Phi \leq 0.20$. On the other hand, the P_W distribution for $\Phi \geq 0.3$ indicates that the combustion region intruded into the constant-area section. At $\Phi = 0.41$, the start point of the pressure rise reached the facility nozzle. For the stinger case, the trend of P_W with Φ shows no remarkable difference with those for the circular case.

Figure 4 indicates the pressure gains at $\Phi = 0.20$ and 0.33. The solid symbols denote the data on the injector-side wall, and the open symbols denote those on the opposite-side wall. Figure 4(a) shows that the multiple arrangement of stinger injectors produced higher pressure thrust ($P_{W,ST}/P_{W,CR} \sim 1.05$) in the diverging section when the combustion region was limited in the diverging section (scramjet operation). The effect of injector-port shape, however, was insignificant to the thrust when the precombustion shock wave formed far upstream of the injectors (dual-mode scramjet operation). Figure 5 illustrates the schematic im-

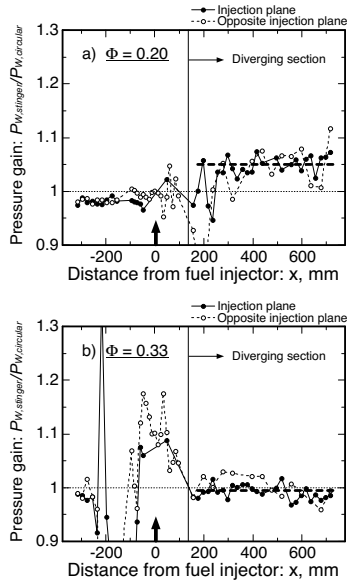


Fig. 4. Pressure gain with multiple stinger injectors at (a) $\Phi = 0.20$ and (b) $\Phi = 0.33$.

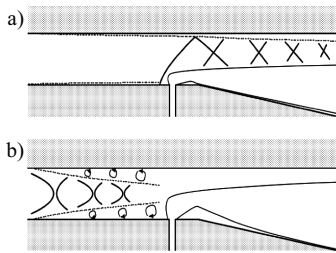


Fig. 5. Schematic flow image of combustors in (a) scramjet mode operation and (b) dual-mode operation.

ages of the flow structures for the scramjet and dual-mode operations. For dual-mode operation, the flow disturbance and effective jet-to-freestream momentum ratio are increased by the flow separation due to the shock train. Highly turbulent incoming flow due to the precombustion shock wave obscured the difference of the injector shape.

For the single injector case, mode transition occurred at $\Phi > 0.5$. This is higher than that for the multiple injector case. For the multiple injector case, the fuel mass flow rate supplied per injector port was lower than that for the single injector case at the same Φ . This induced earlier mode transition and propagation of precombustion shock wave further upstream at a low Φ . We therefore compared the data of the multiple injector case with those of the single injector case having similar pressure distributions with the same combustion mode.

For the single injector case, the pressure gain of the stinger injector was 1.1 at the scramjet mode.⁹⁾ This was higher than that for the multiple injector case ($P_{W,ST}/P_{W,CR} \sim 1.05$). The effect of the injector shape in the multiple injector case was smaller than that for the single injector case. During dual-mode operation, the effect of injector-port shape was insignificant to the thrust even for the single injector case.⁹⁾ This was similar to the result for the multiple injector cases.

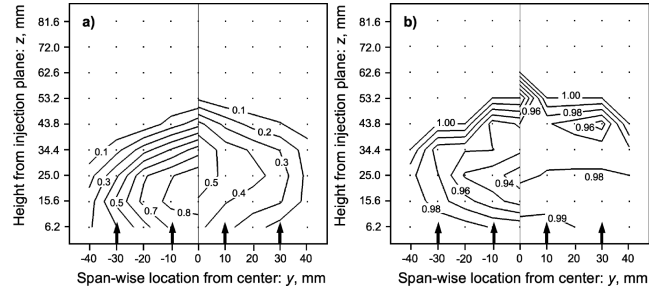


Fig. 6. Distributions of (a) local equivalence ratio and (b) combustion efficiency at the exit of the combustor with multiple circular injectors (left) and multiple stinger injectors (right) at $\Phi = 0.20$.

3.2. Local equivalence ratio and combustion efficiency

Figure 6 presents the exit cross-sectional ϕ and η_c distributions at $\Phi = 0.20$. The left portions of the contour maps are the data for the circular case and the right portions are those for the stinger case. The dots denote the sampling points. For both cases, no individual plumes were identified at the exit of the combustor. The fuel jets merged with each other to make a single plume up to the exit of the combustor. The plumes for the multiple injectors spread more laterally compared to those for the single injector cases.⁹⁾ On the other hand, the vertical penetrations for the multiple injectors were lower than those for the single injector because the fuel flow rate per injector decreased for the same Φ .

A comparison of ϕ for the stinger case with that for the circular case revealed that the vertical penetration for the stinger case was higher than that for the circular case. In addition, the lower ϕ values for the stinger case imply that the multiple arrangement of the stinger injector promoted fuel-air mixing compared to that of the circular injector. This is the main reason why the multiple arrangement of the stinger injector produced 5% higher pressure in the diverging section.

For the multiple injector case, the interaction of each bow shock wave due to fuel injection is one of the key issues to achieve higher combustor performance. When the jet width becomes larger compared to the interval of the injectors, the bow shock waves strongly interact with each other.¹⁴⁾ This induces flow separation. As a result, the airflow rate passing through the adjacent injectors drops. The stinger injector generated a laterally narrow and vertically penetrated jet plume for the low J regime.⁹⁾ The blockage effect for the jets from the multiple stinger injectors would be less than that from the multiple circular injectors. The airflow easily passed between the adjacent stinger injectors. In addition, stinger injectors have a very high length-to-width ratio slit in the stream-wise direction. This promotes large-scale mixing of the fuel plume with the air passing between the adjacent injectors in the same manner as the single injector configuration.⁹⁾

On the other hand, for the multiple circular injector case, a heat mark on the injector block indicates that strong interaction of the bow shock waves occurred at the intervals of the adjacent injectors, leading to flow separation. This separation reduces the airflow passing between the adjacent injectors

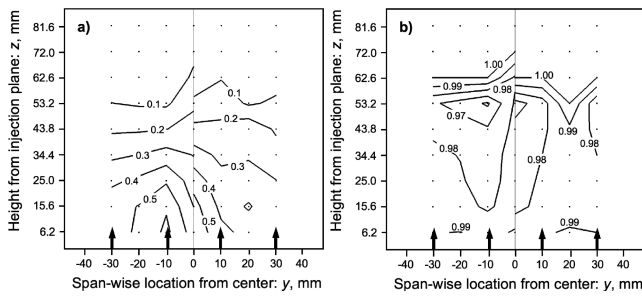


Fig. 7. Distributions of (a) local equivalence ratio and (b) combustion efficiency at the exit of the combustor with multiple circular injectors (left) and multiple stinger injectors (right) at $\Phi = 0.33$.

and decreases combustor performance. Unfortunately, we have no sampling data near the fuel injectors in the combustion case. The low ϕ and higher penetration for the stinger case, however, support the assumption that no large separation occurred in the boundary layer between the adjacent stinger injectors.

The combustion efficiency for the stinger case was over 0.96. Even for the circular case, η_c was over 0.94. The air near the opposite-side wall of the injector was unavailable for combustion for these cases because the fuel plume did not reach the opposite-side wall. If this was modified, for example, additional multiple injectors are placed on the opposite wall, much higher pressure gain would be obtained for the stinger case.

The ability of the stinger shape became impaired for dual-mode scramjet operation when the combustion region intruded into the constant-area section. Figure 7 presents the exit ϕ and η_c distributions at $\Phi \sim 0.33$ when precombustion shock formed and propagated far upstream of the injectors. For both cases, the fuel was uniformly distributed in the span-wise direction, similar to Rogers' experiments.¹³⁾ The high ϕ regions were detected near the injector-side wall, though the fuel penetrated more deeply into the mainstream compared to those at low $\Phi = 0.2$. The ϕ and η_c distributions for the stinger case were not appreciably different from those for the circular case. The injector port shape was insignificant to combustor performance during dual-mode scramjet operation.

4. Conclusion

Four stinger injectors arrayed at $s/D \sim 6.7$ were tested in a Mach 2.44 supersonic combustor with a 1.66° diverging section at $T_0 = 2060$ K. Wall pressure and gas sampling measurements confirmed the ability of the multiple stinger injectors to improve combustor performance. For $\Phi < 0.3$, the combustion region was limited in the diverging section of the combustor, so the combustor was operated in the scramjet mode. For this mode, compared with the airflow between the multiple circular injectors, the airflow much more

easily passed between the adjacent stinger injectors due to the low blockage effect. As a result, the pressure thrust in the stinger case was 5% higher than that in the circular case. The effects of the injector port shape became unclear when the precombustion shock waves appeared far upstream of the injectors (dual-mode scramjet operation). The fuels from the multiple injectors were uniformly distributed in the span-wise direction, and combustor performance was mainly dominated by the change in airflow momentum flux and disturbance due to the precombustion shock wave.

References

- 1) Gruber, M. R., Nejad, A. S., Chen, T. H., and Dutton, J. C.: Transverse Injection from Circular and Elliptic Nozzles into a Supersonic Crossflow, *J. Propul. Power*, **16** (2000), pp. 449–457.
- 2) Barber, M., Schetz, J. A., and Roe, L. A.: Normal, Sonic Helium Injection through a Wedge-Shaped Orifice into Supersonic Flow, *J. Propul. Power*, **13** (1997), pp. 257–263.
- 3) Tomioka, S., Jacobsen, L. S., and Schetz, J. A.: Sonic Injection from Diamond-Shaped Orifices into a Supersonic Crossflow, *J. Propul. Power*, **19** (2003), pp. 104–114.
- 4) Kobayashi, K., Bowersox, R., Srinivasan, R., Carter, C., and Hsu, K.-Y.: Flowfield Studies of Diamond-Shaped Fuel Injector in a Supersonic Flow, *J. Propul. Power*, **23** (2007), pp. 1168–1176.
- 5) Srinivasan, R. and Bowersox, R.: Simulation of Transverse Gaseous Injection through Diamond-Shaped Ports into Supersonic Freestream, *J. Propul. Power*, **23** (2007), pp. 772–782.
- 6) Tomioka, S., Izumikawa, M., Kouchi, T., Masuya, G., Hirano, K., and Matsuo, A.: Matched Pressure Injections into a Supersonic Crossflow through Diamond-Shaped Orifices, *J. Propul. Power*, **24** (2008), pp. 471–478.
- 7) Tomioka, S., Kouchi, T., Masumoto, R., Izumikawa, M., and Matsuo, A.: Supersonic Combustion with Supersonic Injection through Diamond-Shaped Orifices, *J. Propul. Power*, **27** (2011), pp. 1196–1203.
- 8) Hirano, K., Matsuo, A., Kouchi, T., Tomioka, S., and Izumikawa, M.: New Injector Geometry for Penetration Enhancement of Perpendicular Jet into Supersonic Flow, AIAA Paper 2007-5028, 2007.
- 9) Kouchi, T., Masuya, G., Hirano, K., Matsuo, A., and Tomioka, S.: Supersonic Combustion using a Stinger-Shaped Fuel Injector, *J. Propul. Power*, **29** (2013), pp. 639–647.
- 10) Kouchi, T., Hirano, K., Kobayashi, K., Tomioka, S., Izumikawa, M., and Matsuo, A.: Combustion Performance of Supersonic Combustor with Stinger-Shaped Fuel Injector, AIAA Paper 2008-4503, 2008.
- 11) Wagner, J. P., Cameron, J. M. and Billig, F. S.: Penetration and Spreading of Transvers Jets of Hydrogen in a Mach 2.72 Airstream, NASA CR-1794, 1971.
- 12) McClinton, C. R.: The Effect of Injection Angle on the Interaction between Sonic Secondary Jets and a Supersonic Free Stream, NASA TN D-6669, 1972.
- 13) Rogers, R. C.: Mixing of Hydrogen Injected from Multiple Injectors Normal to a Supersonic Airstream, NASA TN D-6476, 1971.
- 14) Sun, M., Lei, J., Wu, H., Liang, J., Liu, W., and Wang, Z.: Flow Patterns and Mixing Characteristics of Gaseous Fuel Multiple Injections in a Non-reacting Supersonic Combustor, *Heat Mass Transfer*, **47** (2011), pp. 1499–1516.
- 15) Mitani, T., Chinzei, N., and Kanda, T.: Reaction and Mixing-Controlled Combustion in Scramjet Engines, *J. Propul. Power*, **17** (2001), pp. 308–314.

T. Watanabe
Associate Editor